Rising Thermal Extremes and Seasonal Particulate Exposure in Western Mato Grosso, Brazil (2000-2025): An Environmental Exposure Profile and the Case for Health Surveillance

Ernandes Sobreira Oliveira Junior[1,*], Maísa Consuelo dos Santos[1], Cleverson Ricardo Soares Viana[1], Daiana Ferreira Dias[1], Adryelle Lemes de Campos[1], Sofia Caumo[2] and Adriana Gioda[3]

[1]Centro de Pesquisa em Limnologia, Biodiversidade e Etnobiologia do Pantanal (CELBE), Laboratório de Investigação Ambiental do Pantanal (LIPAN), Universidade do Estado de Mato Grosso (UNEMAT), Cáceres, Mato Grosso, Brazil

[2]Fundação Oswaldo Cruz (Fiocruz), Rio de Janeiro, Brazil

[3]Departamento de Química, Pontifícia Universidade Católica do Rio de Janeiro (PUC-Rio), Rio de Janeiro, Brazil

Abstract: The western margin of the Pantanal meets the southern edge of the Amazonian deforestation arc, and each dry season its population breathes what the fires leave behind. Yet the small municipalities along this margin are among the least monitored in Brazil, and the exposure their residents carry has never been quantified. We characterised thermal and particulate exposure across 21 municipalities of western Mato Grosso between 2000 and 2025, counting days rather than months above health-relevant thresholds. Daily air temperature, dew point and precipitation came from ERA5-Land; the heat index was computed daily from maximum temperature and the relative humidity concurrent with it, derived from dew point. Fine particulate matter was characterised independently from two validated products, the ACAG satellite-derived estimate (2000-2022) and the NASA GEOS-CF composition reanalysis (2018-2025), and burned area from MODIS MCD64A1. Trends were tested with a Mann-Kendall test modified for serial correlation and the Theil-Sen estimator, with false discovery rate correction across municipalities. Days with a heat index above 39 °C, the NOAA danger level, rose from 8.4 per year in 2000-2009 to 21.4 in 2016-2025; days with maximum temperature above 36 °C rose from 6.5 to 23.1; days with afternoon relative humidity below 30 per cent, the Brazilian meteorological service attention level, rose from 14.1 to 28.7. Maximum temperature rose by 0.394 °C per decade and was significant in all 21 municipalities after correction. Particulate matter showed no trend in either product, but a pronounced seasonal cycle peaking in September at 47.7 and 47.1 μg m^{-3} respectively, closely tracking burned area. Thermal danger and particulate load therefore diverge in direction and are offset in timing, the smoke maximum falling in September and the thermal maximum in October. This is an exposure profile rather than evidence of harm. Even so, a population whose days of thermal danger have more than doubled in a quarter century, and whose dry-season air remains heavily loaded, warrants systematic surveillance of respiratory and cardiovascular outcomes.

Keywords: Pantanal, Thermal extremes, Heat index, Fine particulate matter, Environmental exposure, Health surveillance.

1. INTRODUCTION

The Pantanal breathes through its water. The flood pulse of the Upper Paraguay Basin sets the rhythm of the whole system, and when the rains falter and the air warms, that rhythm shortens. The Northern Pantanal now carries thirteen per cent more days without rain than it did in the 1960s, and holds sixteen per cent less water in the landscape during the dry season than it did a decade earlier (Lazaro *et al*., 2020). Regional models under high emissions project warming of five to seven degrees and rainfall losses near thirty per cent by the end of the century (Marengo *et al*., 2016), while sea-surface-temperature analyses anticipate deeper droughts and sharper extremes (Thielen *et al*., 2020).

National remote sensing already places the Pantanal among the fastest-warming biomes in Brazil (MapBiomas, 2025) Over the same period the biome has lost a large share of its wetland surface to the expansion of pasture and infrastructure, a four-decade trajectory of land-cover change and ecological degradation that raises fire risk and erodes the system's resilience (Sobreira *et al*., 2025).

What has drawn far less attention is what this changing air does to the people who live in it. The western edge of the Pantanal meets the arc of deforestation of southern Amazonia, and each dry season the land there burns. Fine particulate matter below 2.5 micrometres is the main product of that burning and one of the best-documented threats to human health, tied to respiratory and cardiovascular illness and death through oxidative stress and inflammation that reach well beyond the lungs (WHO, 2021). Thermal stress acts through a separate pathway,

*Address correspondence to this author at the Centro de Pesquisa em Limnologia, Biodiversidade e Etnobiologia do Pantanal (CELBE), Laboratório de Investigação Ambiental do Pantanal (LIPAN), Universidade do Estado de Mato Grosso (UNEMAT), Cáceres, Mato Grosso, Brazil;
E-mail: ernandes@unemat.br

Received on 04-07-2026 Accepted on 15-08-2026 Published on 26-08-2026

E-ISSN: 2311-8741/26

and the two frequently coincide during drought and fire seasons; recent evidence indicates that simultaneous exposure to extreme heat and $PM_{2.5}$ is associated with greater mortality than either exposure alone (Rahman *et al*., 2022) Direct evidence of this exposure already exists for the Pantanal itself: firefighters and brigade members monitored during dry-season training in the biome carried a measurable body burden of smoke-related pollutants, with polycyclic aromatic hydrocarbon metabolites elevated in their urine even before the active fire season (Caumo *et al*., 2026).

The evidence from the surrounding Amazon is consistent. A nationwide analysis of more than two million hospital admissions found that wildfire waves raised respiratory admissions by 23 per cent and circulatory admissions by 21 per cent, with effects in the North of the country reaching 38 and 27 per cent respectively (Requia *et al*., 2021). In the Amazon specifically, an increase of one standard deviation in $PM_{2.5}$ has been associated with a 1.5 per cent rise in the monthly respiratory hospitalisation rate (Rocha & Sant'Anna, 2022), and chronic exposure across the Amazonian capitals was estimated to account for some 5 500 circulatory and 2 600 respiratory deaths between 2018 and 2023 (Silveira *et al*., 2026). Causality runs in the expected direction: where upwind protected forest keeps particulate levels down, respiratory hospitalisations fall with them (Sheehan *et al*., 2024).

Even so, the western Pantanal itself has been left largely undescribed. Most of what we know comes from the Amazonian capitals or from the biome treated as a whole, while the small, scattered municipalities of the wetland margin, the ones with the least monitoring, remain a blank. The 2021 revision of the WHO guidelines widened the problem, lowering the annual reference for particulate matter to 5 μg m^{-3} and the 24-hour reference to 15 μg m^{-3}, and opening a gap between what health evidence now recommends and what national standards still permit.

This is the gap we set out to measure, and the way we measure it matters. Monthly means are a poor description of exposure to extremes: a month whose mean maximum temperature is 31 °C may contain ten days above 36 °C, and a threshold applied to the monthly mean discards all ten. We therefore evaluate every threshold at daily resolution and report the number of days on which it was crossed. We set out to describe recent climatic trends across 21 municipalities of western Mato Grosso from 2000 to 2025, to quantify exposure to thermal stress, low humidity and fine particulate matter against health-relevant thresholds counted in days, and to establish whether these exposures move together or apart in trend and in season. We do not test whether this exposure causes disease. Monthly hospital admission and mortality records are available to us for these municipalities, but monthly aggregation cannot separate an environmental signal from the epidemiological seasonality of respiratory disease, and short-term exposure-response analysis requires daily series. We treat the exposure itself as the reason to start watching. To our knowledge, this is the first daily-resolution, threshold-based profile of combined thermal and particulate exposure for the municipalities of the western Mato Grosso margin, a region with no fixed air quality monitoring, and the first to characterise the particulate field there from two independent validated products rather than one. The specific contribution of the study is therefore threefold: an exposure accounting expressed in days rather than in monthly means, a cross-validated description of the seasonal particulate cycle, and the identification of a roughly one-month offset between the smoke maximum and the thermal maximum, which bears directly on the timing of surveillance.

2. MATERIALS AND METHODS

2.1. Study Area

The study covers 21 municipalities of western Mato Grosso, Brazil, distributed between the northern margin of the Pantanal floodplain and the Chapada dos Parecis uplands, along a north-south transect of roughly 500 km bounded to the west by the Bolivian border (Figure **1**). Together they held 315 195 inhabitants at the 2022 Demographic Census. The study area comprises the 21 municipalities of the western region of Mato Grosso (região Oeste), the contiguous block lying between the Pantanal floodplain and the Chapada dos Parecis uplands, bounded to the west by the Bolivian border. Municipal boundaries follow the IBGE municipal mesh, 2018 edition, and each municipality was identified by its seven-digit IBGE code. The set spans the full physiographic gradient of the region, from floodplain to upland, and the complete range of municipal population sizes found across the western region of Mato Grosso.

The region is small in population and highly fragmented administratively. Cáceres, the historic river port on the upper Paraguay and the regional service centre, holds 92 639 inhabitants, and Pontes e Lacerda 55 050; together these two account for almost half the regional population. The remaining municipalities are markedly smaller, with a median population of 6 432, and nine of them have fewer than 5 000 inhabitants. This settlement structure matters for the questions asked here, because environmental monitoring infrastructure follows population. To our knowledge, no fixed continuous air quality monitoring station operates

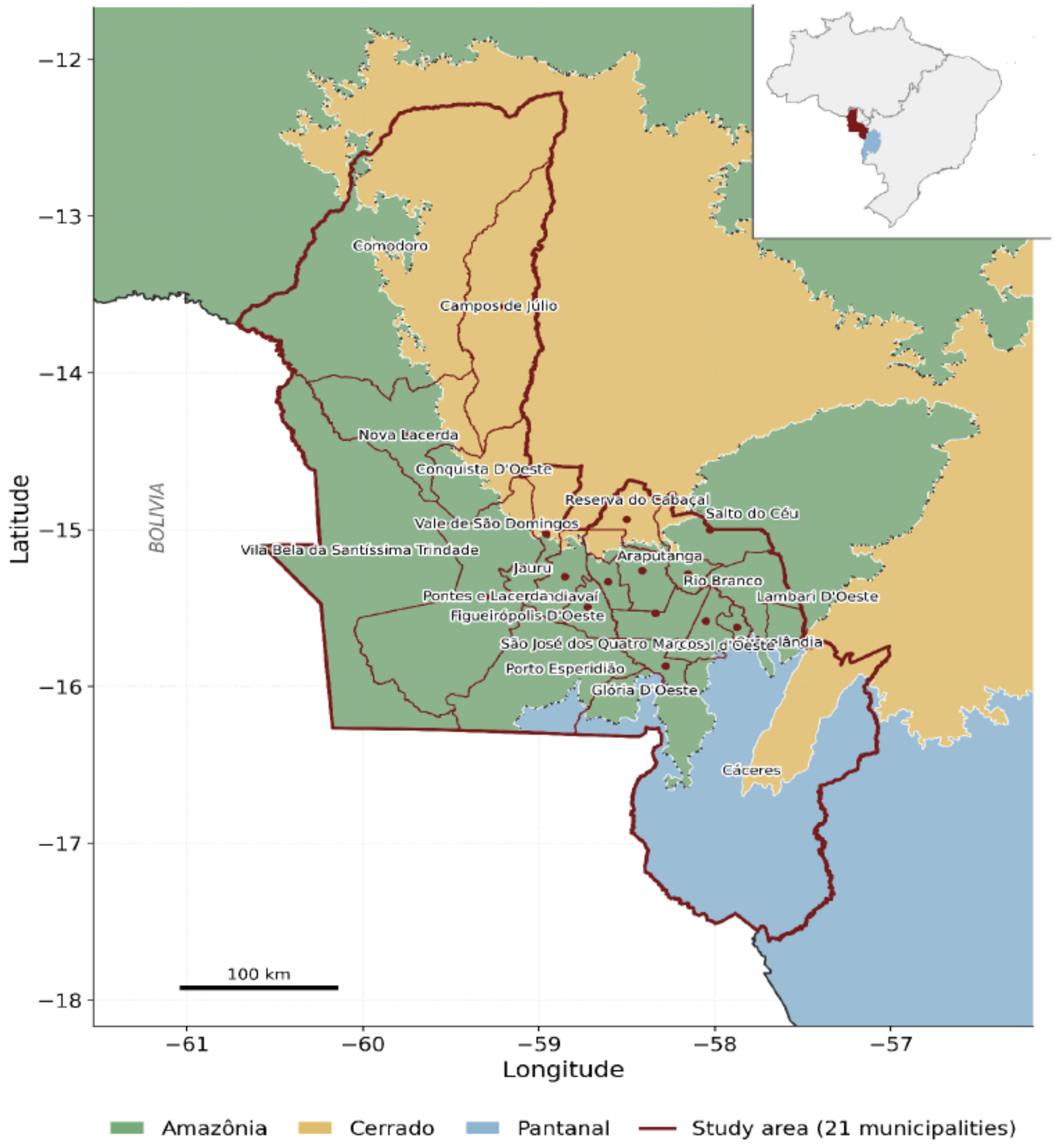

Figure 1: Location of the 21 study municipalities in western Mato Grosso, Brazil. Biome boundaries from IBGE (1:250 000); municipal boundaries from the IBGE 2018 municipal mesh. Source: Authors (2026).

in any of these municipalities. The exposure of this population has therefore never been measured directly, only inferred.

Three biomes converge across the study area. The Pantanal floodplain occupies the southern and eastern portion, the Cerrado the central belt, and the southern fringe of Amazonian forest the north and west, so that the region sits simultaneously on the wetland margin and on the southern edge of the deforestation arc. Hydrologically it is also divided: most municipalities drain eastward into the Upper Paraguay Basin, while the Guaporé valley in the far west, including Vila Bela da Santissima Trindade, drains northward into the Amazon system through the Mamoré and Madeira rivers.

This position generates a marked physiographic gradient that structures much of the variation reported below. Mean maximum air temperature across the study municipalities ranges over 2.5 °C, from the higher ground of the Chapada dos Parecis to the Pantanal lowlands, and mean annual precipitation across the region is approximately 1 370 mm, concentrated between October and April; both figures are derived from the reanalysis series analysed here rather than from station records. Land use follows the same gradient: mechanised soybean and maize production dominates the uplands of the Chapada, while extensive cattle ranching prevails on the lowland plains, with a mosaic of smallholdings and remnant forest along the transition. Both systems use fire, and the dry season between June and October concentrates burning across the whole territory.

2.2. Climatic Variables and Thermal Indices

Daily air temperature, dew point temperature and precipitation were obtained from the ERA5-Land reanalysis (ECMWF/ERA5_LAND/DAILY_AGGR), a global land-surface reanalysis with a spatial resolution of approximately 9 km produced by downscaling of ERA5 (Muñoz-Sabater *et al*., 2021), accessed through Google Earth Engine. Temperatures were converted from kelvin to degrees Celsius. Daily maximum and minimum temperature were taken from the temperature_2m_max and temperature_2m_min bands; daily accumulated precipitation from total_precipitation_sum, converted from metres to millimetres. For each municipality, daily values were extracted in Google Earth Engine as the area-weighted mean of all ERA5-Land grid cells intersecting the municipal polygon, computed at the native resolution of the product, with boundary cells contributing in proportion to their overlapping area. Municipal series are therefore spatial averages rather than point values. At approximately 9 km resolution the smallest municipalities are covered by few grid cells, some of them shared with neighbours, so that series from adjacent small municipalities are not fully independent of one another; the regional series, which averages across all 21 municipalities, is insensitive to this, but municipal-level results for the smallest units should be read as local conditions smoothed to the scale of the reanalysis grid.

Relative humidity is not provided directly and was derived from temperature and dew point using the Magnus-Alduchov-Eskridge formulation of saturation vapour pressure (Lawrence, 2005). Because relative humidity varies by roughly a factor of two between night and afternoon while dew point is nearly conserved through the day, we computed the relative humidity concurrent with the daily maximum temperature as the ratio of saturation vapour pressure at the daily mean dew point to that at the daily maximum temperature. In a tropical climate this quantity corresponds closely to the daily minimum relative humidity, which occurs in the afternoon together with peak temperature, and it is the quantity relevant to both thermal stress and respiratory irritation. The Magnus formulation reproduces saturation vapour pressure to within a fraction of one per cent over the temperature range observed here (Lawrence, 2005), so the derivation rests less on the vapour pressure formula than on one central assumption: that the daily mean dew point represents the dew point prevailing at the hour of maximum temperature. Dew point is far more conservative through the diel cycle than temperature, but it is not constant, and dry-season entrainment of dry air into the deepening boundary layer can pull the afternoon dew point below the daily mean. Where that happens our estimate overstates afternoon relative humidity, which understates the count of low-humidity days and, since the heat index rises with humidity at high temperature, may overstate the heat index. Absolute exceedance counts should be read with this in mind. The derivation, however, is applied identically to every day of the record, so a stable approximation of this kind displaces levels rather than trends, and the trend estimates on which the conclusions of this study rest are insensitive to it.

The heat index was computed daily using the Rothfusz regression adopted by the United States National Weather Service, with the official low-humidity and high-humidity adjustments, taking as input the daily maximum temperature and the concurrent relative humidity defined above. Computing the heat index from monthly means of temperature and humidity, rather than from concurrent daily values, produces substantially different results because the function is non-linear and because monthly mean humidity is not the humidity prevailing at peak temperature; we therefore evaluated it at daily resolution throughout. Using daily mean dew point is a close approximation to afternoon conditions, since dew point is nearly conserved through the day, but it is not equivalent to computation from hourly fields.

2.3. Threshold Exceedance

Each threshold was evaluated for every day and summed to the month, so that all exposure metrics are expressed as numbers of days. Heat index thresholds follow the NOAA classification: 27 °C (caution), 32 °C (extreme caution) and 39 °C (danger). Maximum temperature thresholds of 32, 34 and 36 °C follow the tradition of absolute-threshold warm-day indices used by the Expert Team on Climate Change Detection and Indices. Relative humidity thresholds of 30, 20 and 12 per cent correspond to the state of attention, alert and emergency defined by the Brazilian National Institute of Meteorology for low-humidity conditions.

Because the NOAA heat index bands were developed for a temperate, non-acclimatised population, the lower bands are crossed on most days of the year in this tropical setting and carry limited discriminatory value. We therefore anchor the analysis on the rare and unambiguous indicators, namely heat index above 39 °C, maximum temperature above 36 °C, and relative humidity below 30 and 20 per cent. The lower thresholds are reported as descriptive context only. Throughout, we report trends rather than absolute risk: the thresholds serve as fixed reference points against which change over time can be measured, not as a classification of individual risk in an acclimatised tropical population. This distinction between meteorological exceedance and demonstrated health risk deserves emphasis. The Rothfusz regression approximates Steadman's apparent temperature for a reference population that is not acclimatised to sustained tropical heat, and the choice of heat index algorithm itself affects the values obtained (Anderson *et al*., 2013). Epidemiological evidence shows that the temperature of minimum mortality is not a fixed value but tracks the local climate, sitting near the 60th percentile of the local temperature distribution in tropical locations against the 80th to 90th percentile in temperate ones (Gasparrini *et al*., 2015), so a population long resident in western Mato Grosso is unlikely to experience risk at the same absolute values as the population for which the NOAA bands were calibrated. Exceedance of a threshold documents the physical environment, not a health response; whether the rising frequency of such days translates into morbidity or mortality in this acclimatised population is precisely the question that the surveillance proposed in Section 4.1 would answer.

2.4. Fine Particulate Matter

Fine particulate matter was characterised independently from two products, reported separately and never merged into a single series. The first is the ACAG global satellite-derived $PM_{2.5}$ estimate (Shen *et al*., 2024), which combines aerosol optical depth retrievals from MODIS, MISR, SeaWiFS and VIIRS with GEOS-Chem chemical transport simulation and applies geographically weighted regression against ground monitors, achieving cross-validated agreement of R^2 = 0.90-0.92 with surface measurements; it is available monthly at 0.01° resolution and was used for 2000-2022. The second is the NASA GEOS-CF composition reanalysis (PM25_RH35_GCC), an hourly modelled field at 0.25° resolution, aggregated here to daily means and used for 2018-2025.

We deliberately avoided deriving $PM_{2.5}$ from aerosol optical depth by a fixed conversion factor. Aerosol optical depth measures light extinction by the whole atmospheric column and is strongly inflated by hygroscopic growth at high relative humidity; converting it to surface mass concentration without correcting for water uptake, vertical profile and aerosol composition introduces a humidity-correlated bias that is largest precisely in the wet season, compressing the seasonal amplitude and obscuring the biomass-burning signal. Both products used here incorporate these corrections internally and have been validated against surface measurements.

The two products differ in resolution by more than an order of magnitude. GEOS-CF at 0.25° corresponds to grid cells of roughly 770 km², larger than several of the study municipalities, and should be read as describing regional rather than municipal exposure. ACAG at 0.01° resolves municipal boundaries but ends in 2022. These differences shape what each product can and cannot say. The coarse grid of GEOS-CF averages away any sub-regional gradient, so spatial homogeneity in that product is partly imposed by its resolution rather than demonstrated by it; conversely, its daily fields resolve the timing of smoke episodes that the monthly ACAG product cannot. The observation periods also differ in fire regime, since the ACAG record includes the years of higher burned area at the start of the record (Section 3.3) while GEOS-CF begins in 2018, so the annual means of the two products describe different periods and are not directly comparable with each other. For these reasons the products are compared only over their common interval, 2018-2022, at the municipality-month scale, and quantitative statements are anchored on the dry-season maximum, where the two agree.

2.5. Burned Area

Monthly burned area was obtained from the MODIS MCD64A1 version 6.1 product at 500 m resolution (Giglio *et al*., 2018), counting pixels with a valid burn date and converting to hectares. The product begins in November 2000, so the year 2000 was excluded from the fire analysis, which covers 2001-2025.

2.6. Statistical Analysis

ERA5-Land assimilates observations but remains a model product, and at approximately 9 km resolution the smallest municipalities are represented by few grid cells; results should be read accordingly. For the same reason, the count of municipalities in which a trend is individually significant after false discovery rate correction should be read as a description of spatial coherence rather than as a tally of independent confirmations, since neighbouring municipal series share grid cells and regional variability. Trends were tested on annual series with the Mann-Kendall test modified for serial correlation following Hamed and Rao (1998), since untreated autocorrelation in climatic series inflates apparent significance. Slope magnitude and its 95 per cent confidence interval were estimated with the Theil-Sen estimator. Where the same test was applied across the 21 municipalities or across multiple indicators, p-values were adjusted for multiple comparisons by the Benjamini-Hochberg false discovery rate procedure. Seasonal relationships between variables were assessed with Spearman rank correlation computed on the twelve monthly climatological means. Regional series were built by averaging intensive quantities across municipalities and summing extensive ones. Analyses were performed in Python 3.12 with pymannkendall, SciPy and statsmodels.

Each claim is anchored to a single product over its complete period. Climatic trends rest on ERA5-Land for 2000-2025; particulate characterisation on ACAG for

2000-2022 and GEOS-CF for 2018-2025, cross-validated over the common interval; burned area on MCD64A1 for 2001-2025. No trend is computed across a spliced series.

3. RESULTS

3.1. Climatic Trends

Temperature rose across the study region over the 26 years examined, and the signal is unambiguous. Maximum air temperature increased by 0.394 °C per decade (95 % CI 0.148 to 0.715; $p = 0.005$), amounting to roughly 0.98 °C over the period. Minimum temperature rose more slowly, by 0.263 °C per decade (95 % CI 0.069 to 0.491; $p = 0.009$), so that daytime warming exceeded night-time warming, although the confidence intervals overlap and the difference should not be over-read. The heat index rose by 0.401 °C per decade (95 % CI 0.179 to 0.838; $p = 0.003$), slightly faster than maximum temperature itself.

The warming was regionally uniform. Municipal Theil-Sen slopes for maximum temperature ranged narrowly from 0.332 to 0.506 °C per decade, with a median of 0.393, and the trend was significant in all 21 municipalities after false discovery rate correction. What variation there is tracks the physiographic gradient rather than any municipal characteristic: the lowland Pantanal municipalities, which are also the warmest, warmed somewhat faster than the Chapada dos Parecis uplands.

Neither humidity nor rainfall carried a reliable trend. Relative humidity concurrent with maximum temperature declined by 1.31 percentage points per decade but the test did not reach significance (95 % CI −2.91 to +0.25; $p = 0.219$), and mean relative humidity behaved similarly (−1.82 points per decade; $p = 0.166$). Total precipitation showed no trend (−38.7 mm per decade; 95 % CI −156 to +72; $p = 0.378$). The region has therefore warmed without a detectable change in its moisture regime over this period.

3.2. Threshold Exceedance and its Trends

Counting days rather than months changes the picture substantially, and every thermal and hygric indicator rose significantly (Table **1**). The rare extremes give the clearest signal. Days with a heat index above 39 °C, the NOAA danger level, averaged 8.4 per municipality per year in 2000-2009 and 21.4 in 2016-2025, a rise of 6.44 days per decade (95 % CI 2.17 to 11.91; $p < 0.001$). Days with maximum temperature above 36 °C rose from 6.5 to 23.1 over the same comparison, at 7.92 days per decade (95 % CI 2.98 to 14.33). Days of thermal danger have therefore more than doubled within a single generation.

Low humidity followed the same direction. Days with afternoon relative humidity below 30 per cent, the attention level of the Brazilian meteorological service, rose from 14.1 to 28.7 per year, at 8.07 days per decade (95 % CI 0.98 to 17.45; $p = 0.017$). Days below the 20 per cent alert level remain rare, averaging 0.1 per year in 2000-2009 against 2.5 in 2016-2025. For this indicator the decadal contrast and the Theil-Sen slope in Table **1**, +0.10 days per decade with a confidence interval reaching zero, answer different questions and should not be read against each other. In a zero-inflated series in which most years record no exceedance at all, the Theil-Sen estimator, being the median of pairwise slopes, is dominated by pairs of years with zero or near-zero counts and stays close to zero, while the decadal means are driven by a small number of recent extreme years. The rank-based Mann-Kendall test detects the monotonic accumulation of non-zero years ($p = 0.006$), but the slope for this indicator is a conservative lower bound on the change. We therefore read the 20 per cent indicator as evidence that a formerly rare condition has begun to recur, not as a quantified rate of increase. No day in the record fell below the 12 per cent emergency level in any municipality.

The lower NOAA bands are reported for completeness but discriminate little: the caution level of 27 °C is crossed on 326 days per year and the extreme-caution level of 32 °C on 211, so that most of the year already sits within them. Their trends are positive and significant, but the interpretive weight belongs to the rarer thresholds.

Eight of the nine indicators remained significant after false discovery rate correction across indicators; only the 12 per cent humidity emergency level, which was never crossed, did not.

3.3. Fine Particulate Matter

The two particulate products agree on the shape and magnitude of the dry-season maximum and disagree on the wet-season floor (Table **2**). ACAG gives a regional annual mean of 19.1 μg m^{-3} for 2000-2022 with a September mean of 47.7; GEOS-CF gives 14.4 μg m^{-3} for 2018-2025 with a September mean of 47.1. Over the common interval the two are strongly correlated (Pearson $r = 0.895$, $n = 1260$), but the rank correlation is considerably weaker (Spearman $r = 0.482$), indicating that the agreement is driven by the extreme values while the products diverge across the ordinary range. The practical implication of this divergence deserves to be stated. The cross-validation supports the magnitude and the timing of the dry-season maximum, where the health-relevant concentrations occur and where the two products

Table 1: Threshold exceedance across 21 municipalities of western Mato Grosso, 2000-2025, expressed as days per municipality per year. Trends from the Theil-Sen estimator; significance from the Mann-Kendall test modified for serial correlation, with Benjamini-Hochberg correction across indicators. For zero-inflated indicators, relative humidity below 20 and 12 per cent, the Theil-Sen slope is a conservative lower bound on the change; see Section 3.2.

Indicator	Days/yr 2000-2025	2000-2009	2016-2025	Trend (days/decade)	95 % CI	p (FDR)
Heat index > 39 °C (danger, NOAA)	14.4	8.4	21.4	+6.44	2.17 - 11.91	< 0.001
Maximum temperature > 36 °C	14.4	6.5	23.1	+7.92	2.98 - 14.33	0.004
Relative humidity < 20 % (alert, INMET)	1.3	0.1	2.5	+0.10	0.00 - 0.53	0.006
Maximum temperature > 34 °C	42.1	29.7	56.4	+12.98	5.00 - 24.59	0.006
Relative humidity < 30 % (attention, INMET)	21.6	14.1	28.7	+8.07	0.98 - 17.45	0.017
Heat index > 32 °C (extreme caution)	211.3	200.6	225.8	+14.66	3.43 - 27.16	0.014
Maximum temperature > 32 °C	104.9	89.7	125.6	+18.74	5.50 - 34.38	0.013
Heat index > 27 °C (caution)	326.2	321.7	330.5	+5.99	1.05 - 11.19	0.015
Relative humidity < 12 % (emergency)	0.0	0.0	0.0	0.00	n.a.	1.000

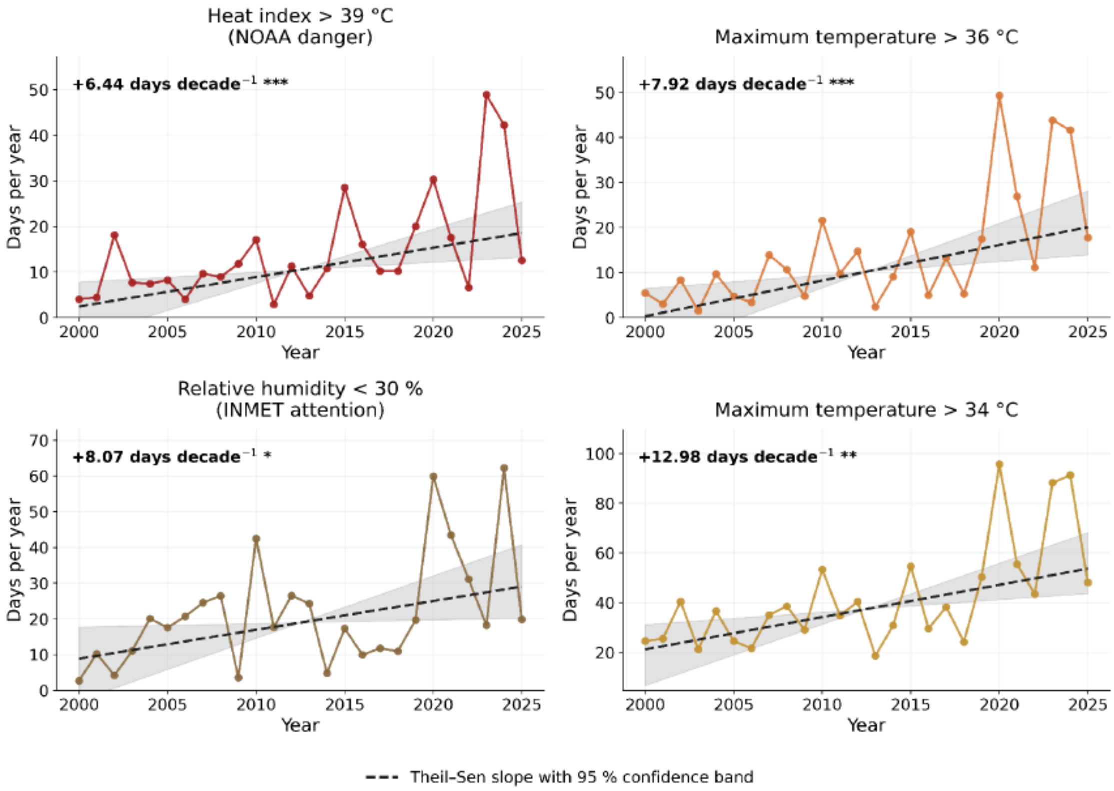

Figure 2: Annual number of days above selected thermal and hygric thresholds, averaged across the 21 study municipalities, 2000-2025. Dashed lines show Theil-Sen slopes with 95 % confidence bands. Asterisks denote significance under the Mann-Kendall test modified for serial correlation: * $p < 0.05$, ** $p < 0.01$, *** $p < 0.001$. The confidence bands are wide because interannual variability in this region is large relative to the trend, driven by the El Niño-Southern Oscillation and by year-to-year variation in the onset of the rains. Significance is established by the rank-based Mann-Kendall test with correction for serial correlation, which assesses the monotonicity of the series and is robust to this dispersion, rather than by the width of the interval around the slope.

converge, but it does not validate either product across the ordinary range: a municipality-month classified as moderately polluted by one product may be ranked quite differently by the other. Any analysis that depends on the ordering of low and intermediate values, such as exposure classification outside the burning season, would be product-dependent, and we do not attempt one here.

That divergence is concentrated in the wet season. ACAG places the March mean at 14.9 µg m^{-3} and GEOS-CF at 5.6, giving seasonal amplitudes of 3.2

Table 2: Fine particulate matter characterised independently from two validated products. Cross-validation over the common interval 2018-2022: Pearson r = 0.895, Spearman r = 0.482 (n = 1260 municipality-months)

Product	Period	Resolution	Annual mean ($\mu g\ m^{-3}$)	September	March	Sep/Mar	Trend ($\mu g\ m^{-3}$/decade)	p
ACAG V6.GL.02	2000-2022	0.01° (~1 km)	19.1	47.7	14.9	3.2	−2.12	0.154
NASA GEOS-CF v1	2018-2025	0.25° (~27 km)	14.4	47.1	5.6	8.3	−3.12	0.711

and 8.3 respectively. Field measurements from the Amazonian burning arc report fine particulate near 2.5 $\mu g\ m^{-3}$ outside fire events and 33 to 44 $\mu g\ m^{-3}$ during the burning season, which places the GEOS-CF wet-season floor closer to observation. We therefore report both and anchor quantitative statements on the dry-season maximum, where the two converge. Where they diverge, the Amazonian field measurements favour GEOS-CF at the wet-season floor, while at the dry-season peak the products agree to within one microgram per cubic metre.

Neither product shows a trend. ACAG gives −2.12 $\mu g\ m^{-3}$ per decade (95 % CI −5.32 to +0.84; p = 0.154) and GEOS-CF −3.12 (95 % CI −21.18 to +28.47; p = 0.711) over its shorter and consequently far less constrained record. Burned area over 2001-2025 likewise declined, though only marginally (−11 788 ha per year; p = 0.065), from a mean of 493 000 ha per year in 2001-2009 to 416 000 in 2017-2025.

3.4. Seasonality

All exposures concentrate between August and October, but they do not peak together (Table **3**). Low humidity peaks first, in August, with 10.9 days below 30 per cent. Particulate matter and burned area peak in September, at 47.7 $\mu g\ m^{-3}$ and 7533 ha respectively, and their seasonal cycles track each other closely (Spearman r = 0.881 for GEOS-CF, 0.594 for ACAG, computed on the twelve monthly means). Low humidity tracks fire even more tightly (r = 0.911). These are seasonal covariations, not attributions: burning, low humidity and high particulate load are joint expressions of the same dry season, and the particulate field over any one municipality reflects regional transport from burning across and beyond the study area as much as fire within it. Thermal danger peaks last, in October, with 4.93 days above the 39 °C heat index level against 2.29 in September.

Thermal danger and particulate load are therefore offset by roughly one month and essentially uncorrelated across the seasonal cycle (Spearman r = 0.210). The dry season therefore delivers two distinct exposures in sequence rather than a single compound hazard. Smoke and low humidity come first, in August and September; thermal extremes follow in September and October. This sequential structure describes the

Table 3: Monthly climatology of exposure indicators across 21 municipalities. Thermal and hygric indicators 2000-2025; ACAG 2000-2022; GEOS-CF 2018-2025; burned area 2001-2025. Thermal indicators, hygric indicators and burned area are expressed as monthly means per municipality; $PM_{2.5}$ values are regional monthly means. The regional burned-area totals reported in Section 3.3 are the sums of these per-municipality values across the 21 municipalities

Month	HI > 39 °C (days)	Tmax > 36 °C (days)	RH < 30 % (days)	$PM_{2.5}$ ACAG ($\mu g\ m^{-3}$)	$PM_{2.5}$ GEOS-CF ($\mu g\ m^{-3}$)	Burned area (ha)
January	1.12	0.04	0.00	14.9	6.1	106
February	0.88	0.01	0.00	14.3	5.7	183
March	0.95	0.02	0.00	14.9	5.6	273
April	0.32	0.00	0.00	11.6	5.9	146
May	0.00	0.00	0.02	10.7	7.8	266
June	0.00	0.00	0.15	12.3	10.0	504
July	0.00	0.00	3.54	11.4	10.5	1 164
August	0.07	2.46	10.91	26.6	26.9	5 355
September	2.29	6.72	5.75	47.7	47.1	7 533
October	4.93	3.77	0.70	30.0	26.4	3 292
November	2.28	1.16	0.49	17.9	13.3	1 154
December	1.53	0.17	0.01	17.0	7.7	392

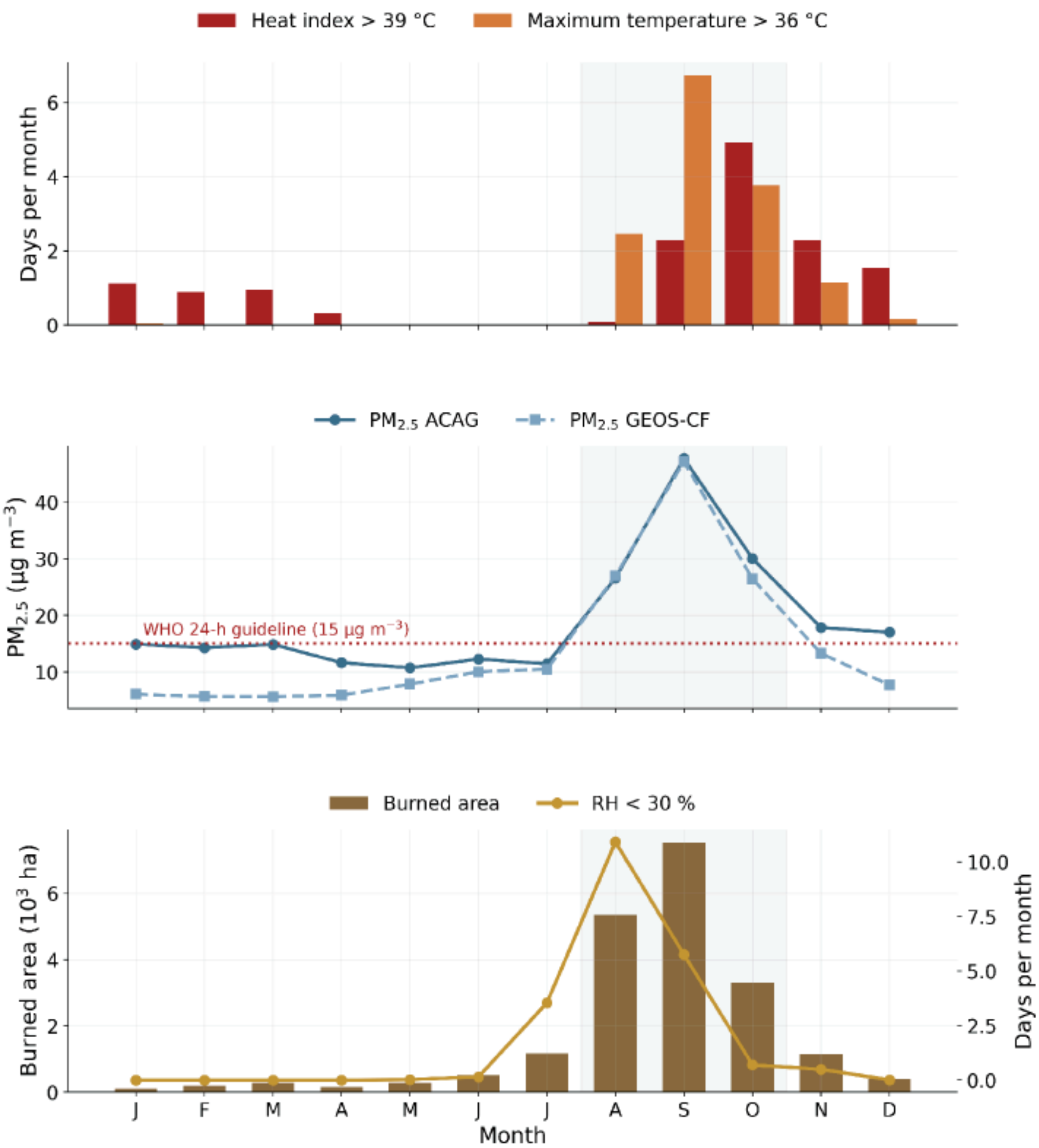

Figure 3: Monthly climatology of exposure indicators. Top: days above thermal thresholds. Middle: $PM_{2.5}$ from two independent products, with the WHO 24-hour guideline for reference. Bottom: burned area and days with afternoon relative humidity below 30 per cent. The shaded band marks August to October. The humidity and particulate maxima precede the thermal maximum by roughly one month.

hazard more precisely than a combined index would, and it says when surveillance effort should be concentrated.

3.5. Spatial Pattern

Thermal danger is concentrated in the lowland municipalities. Cáceres records 51.6 days per year with a heat index above 39 °C, followed by Glória d'Oeste (38.3), Lambari d'Oeste (33.8), Curvelândia (31.9) and São José dos Quatro Marcos (22.8). The trend is upward and significant after correction in all 21 municipalities, ranging from 8.2 to 16.6 additional danger days per decade. This ranking follows elevation and baseline temperature rather than any demographic or land-use characteristic, and it should be interpreted as a physiographic pattern.

Particulate exposure, by contrast, shows little municipal differentiation in the products analysed. Part of this homogeneity is likely real, since smoke from biomass burning is transported over hundreds of kilometres and mixes across a territory of this extent; part of it is imposed by the data, since a single GEOS-CF grid cell spans several municipalities and cannot register sub-grid contrasts, and no ground monitor exists against which local gradients, such as urban plumes or the vicinity of individual fires, could be detected. The apparent uniformity should be read as an absence of resolvable contrast at the scale of the products, not as evidence that all residents experience the same concentrations. Municipal differentiation in this study therefore derives almost entirely from thermal exposure.

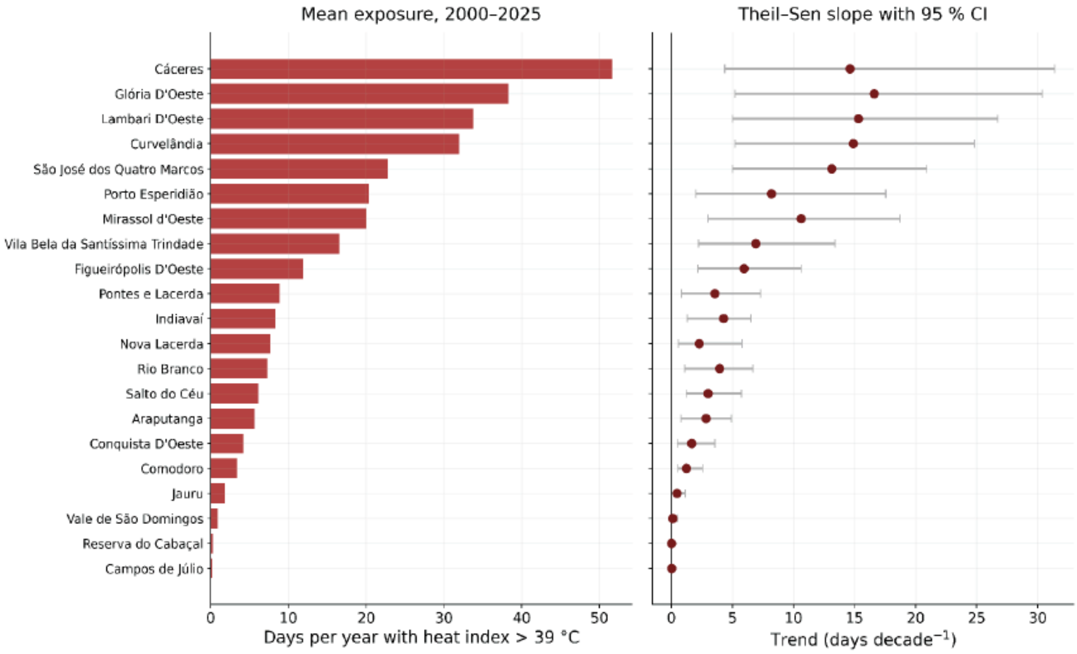

Figure 4: Thermal danger by municipality. Left: mean annual number of days with a heat index above 39 °C, 2000-2025. Right: Theil-Sen trend with 95 % confidence interval. The ranking follows the physiographic gradient from the Chapada dos Parecis uplands to the Pantanal lowlands.

4. DISCUSSION

The region has warmed uniformly and significantly, with daytime maxima rising faster than nocturnal minima. Days of thermal danger have more than doubled between the first and last decade of the record, and days of critically low humidity have doubled. Fine particulate matter behaves differently: it shows no trend in either of two independent products, yet retains a pronounced dry-season maximum that closely tracks burned area.

These two exposures call for different responses. A warming signal that is monotonic and spatially uniform is a slow accumulation in baseline conditions. A particulate load that is stationary in trend but sharply seasonal is a recurring annual event with predictable timing. That they peak a month apart matters practically: August and September bring smoke and desiccating air, September and October the thermal extremes. A single composite hazard index would blur this structure rather than reveal it. We also note that the correspondence between burned area, low humidity and particulate load is described throughout as covariation within the dry season, not as a causal chain estimated from these data. Separating the contributions of local burning, regional transport from the Amazonian and Cerrado burning arcs, and the meteorology that modulates both, notably boundary-layer depth and atmospheric stagnation, would require dispersion modelling or source apportionment beyond the scope of an exposure profile.

The absence of a particulate trend, together with a marginal decline in burned area, is not an improvement in air quality. Burning-season concentrations remain far above the WHO 24-hour guideline of 15 μg m^{-3} in every municipality, and annual means from both products exceed the 5 μg m^{-3} annual guideline threefold to fourfold. The burden is persistent rather than worsening, and it sits beneath a thermal burden that is worsening.

One methodological point applies well beyond this region. Evaluating thresholds on monthly means rather than daily values does not merely blur the estimate; it can eliminate the phenomenon. Applied to monthly means in these municipalities, the Brazilian alert threshold for low humidity is never crossed in 26 years. Applied daily, it is crossed on 1.3 days per year and rising, and the attention threshold on 21.6 days per year. Where exposure to extremes is the object of study, the temporal resolution at which thresholds are evaluated determines the result.

4.1. Implications for Environmental Health Surveillance

Everything in this section is prospective. Nothing documented above demonstrates that the exposures described have produced illness in these municipalities; the associations between heat, fine particulate matter and respiratory or cardiovascular outcomes invoked below were established in other populations, and their transfer to western Mato Grosso is the hypothesis that surveillance would test, not a finding of this study. Although the environmental indicators were evaluated at the municipal level, the observed patterns reflect broader regional climatic processes rather than isolated local conditions. Air temperature, atmospheric moisture and particulate matter are governed by atmospheric circulation and seasonal dynamics that extend across administrative boundaries. Environmental exposure should therefore be interpreted as a regional phenomenon, whereas public health preparedness frequently remains organised through fragmented municipal structures.

This mismatch between the spatial scale of environmental processes and the administrative scale of decision-making represents an important challenge for climate adaptation (Bonnett & Birchall, 2023). Municipal health systems often respond independently to environmental risks that originate from regional climatic drivers, limiting opportunities for coordinated surveillance and resource allocation. As climatic extremes become more frequent, isolated municipal responses may prove insufficient to address exposures that simultaneously affect multiple jurisdictions (Buzási *et al*., 2024).

Rather than relying exclusively on traditional epidemiological indicators, environmental health surveillance could progressively incorporate climatic and atmospheric information as complementary sources of evidence (Morin *et al*., 2018). Such an approach shifts surveillance from a predominantly reactive model toward one that emphasises anticipation and preparedness.

In practical terms, surveillance in western Mato Grosso could integrate daily maximum temperature, heat index, relative humidity, $PM_{2.5}$ concentration and fire occurrence with healthcare indicators including outpatient visits, emergency department attendances and hospital admissions for respiratory and cardiovascular conditions. The seasonal structure documented here suggests a specific allocation of effort: particulate and low-humidity monitoring from July through September, and thermal monitoring from September through November. Implementation would require coordination across the levels of Brazil's Unified Health System and the institutions responsible for environmental monitoring, and could be integrated into the national Environmental Health Surveillance Programme for Populations Exposed to Atmospheric Pollutants (Vigiar).

The recommendations presented here derive from an environmental exposure profile and should not be interpreted as a validated early-warning system. Their implementation would depend on the integration of environmental and health data, the establishment of operational alert thresholds, and evaluation of whether periods of elevated environmental exposure coincide with increased demand for healthcare services.

5. LIMITATIONS

Several limitations qualify these results, and we state them explicitly. The first is that no ground measurements exist against which to validate either the climatic reanalysis or the two particulate products within the study region, since no monitoring network operates there. This is the condition that motivated the study, and it is also what the study cannot overcome. The two particulate products agree closely on the dry-season maximum, which is where our quantitative claims are anchored, but diverge by nearly a factor of three in the wet season, and we report both rather than choosing between them. The second limitation follows from the nature of the products themselves. ERA5-Land assimilates observations into a land-surface model and carries structural uncertainty that cannot be quantified over this region for lack of stations; the two particulate products are, respectively, a statistical fusion of satellite retrievals with a chemical transport model and a composition reanalysis, and each embeds model error that their published global validations cannot localise to western Mato Grosso; and the relative humidity used here is itself a derived quantity that approximates afternoon conditions from the daily mean dew point (Section 2.2). None of these uncertainties can be bounded locally without measurements. What can be said is that they weigh on levels more than on trends, because each product is internally consistent through time and every threshold is applied uniformly across the record. The third limitation is spatial aggregation. Municipal values are means over few reanalysis grid cells for the smallest municipalities, one GEOS-CF cell spans several of them, and municipal series are consequently not mutually independent, so municipal contrasts, particularly in particulate exposure, are unresolvable partly by construction (Sections 2.2 and 3.5). The fourth is that every health-related threshold applied here, the NOAA heat index bands, the INMET humidity levels and the WHO particulate guidelines, was developed outside this population, and risk thresholds are known to shift with acclimatisation (Gasparrini *et al*., 2015); the thresholds function in this study as fixed rulers against which change is measured, not as validated local risk levels (Section 2.3).

The last limitation, and the most important, is that this is a description of exposure, not of harm. Monthly hospital admission and mortality records for these municipalities are available to us, but monthly aggregation cannot separate an environmental signal from the marked epidemiological seasonality of respiratory disease, nor detect the short-term effects that matter most for heat and smoke. Establishing whether this exposure translates into demand on the health system requires daily series, and is the next step rather than a caveat on this one.

6. CONCLUSION

Across 21 municipalities of western Mato Grosso, days of thermal danger have more than doubled in a quarter of a century, from 8.4 to 21.4 per year, and days of critically low humidity have doubled. Maximum temperature rose by 0.394 °C per decade, significantly and in every municipality examined. Fine particulate matter has not increased, but remains far above health guidelines through a dry season whose smoke maximum falls in September, one month before the thermal maximum.

These figures describe exposure, not harm. Set beside consistent evidence from the surrounding Amazon that such exposure damages respiratory and cardiovascular health, they are enough to justify systematic surveillance. The exposure is now mapped, and mapped at a resolution that shows when in the year it falls. Linking it to health outcomes, with data sensitive enough to detect an effect, is the work that follows.

AUTHOR ORCID IDENTIFIERS

Ernandes Sobreira Oliveira Junior - https://orcid.org/0000-0002-6953-6917 - ernandes@unemat.br

Maísa Consuelo dos Santos - https://orcid.org/0009-0009-2592-8941 - maisa.shimokawa@unemat.br

Cleverson Ricardo Soares Viana - https://orcid.org/0000-0003-3448-8684 - cleverson.viana@unemat.br

Daiana Ferreira Dias - https://orcid.org/0000-0001-8733-8108 - daiana.dias@unemat.br

Adryelle Lemes de Campos - https://orcid.org/0000-0002-7307-6124 - adryelle.campos@unemat.br

Sofia Caumo - https://orcid.org/0000-0001-7471-4936 - sofia.caumo@gmail.com

Adriana Gioda - https://orcid.org/0000-0002-5315-5650 - agioda@puc-rio.br

CREDIT AUTHORSHIP CONTRIBUTION STATEMENT

Ernandes Sobreira Oliveira Junior: Conceptualization, Methodology, Software, Formal analysis, Investigation, Data curation, Writing - original draft, Writing - review and editing, Visualization, Supervision, Project administration. Maísa Consuelo dos Santos: Data curation, Validation, Investigation, Writing - original draft, Writing - review and editing. Cleverson Ricardo Soares Viana: Data curation, Investigation, Resources, Writing - original draft, Writing - review and editing. Daiana Ferreira Dias: Data curation, Investigation, Resources, Writing - original draft, Writing - review and editing. Adryelle Lemes de Campos: Investigation, Data curation, Writing - original draft, Writing - review and editing. Sofia Caumo: Investigation, Data curation, Writing - original draft, Writing - review and editing. Adriana Gioda: Conceptualization, Writing - review and editing. In practical terms, all authors contributed to data collection and to writing the manuscript. All authors read and approved the final version.

FUNDING

This research received no specific grant from any funding agency in the public, commercial or not-for-profit sectors. The work was carried out using the institutional resources of the Universidade do Estado de Mato Grosso (UNEMAT).

DECLARATION OF COMPETING INTERESTS

The authors declare that they have no known competing financial interests or personal relationships that could have appeared to influence the work reported in this article.

DATA AND CODE AVAILABILITY

All environmental data derive from publicly available products: ERA5-Land (ECMWF), ACAG $PM_{2.5}$ (Washington University in St. Louis), NASA GEOS-CF, and MODIS MCD64A1. The extraction scripts (Google Earth Engine JavaScript) and the analysis code (Python) are available from the corresponding author on request and will be deposited in a public repository upon acceptance.

DECLARATION OF GENERATIVE AI USE

During the preparation of this work, the authors used Claude (Anthropic) to assist with code development, critical review of earlier drafts and language editing. All data extraction and all statistical analyses were designed and executed by the authors, who reviewed and verified every numerical value reported and take full responsibility for the content, the interpretation and the conclusions of this article. No AI system is listed as an author.

REFERENCES

[1] Anderson, G. B., Bell, M. L., & Peng, R. D. (2013). Methods to calculate the heat index as an exposure metric in environmental health research. Environmental Health Perspectives, 121(10), 1111-1119. https://doi.org/10.1289/ehp.1206273

[2] Bonnett, N. L., & Birchall, S. J. (2023). The influence of regional strategic policy on municipal climate adaptation

planning. Regional Studies, 57(1), 141-152. https://doi.org/10.1080/00343404.2022.2049224

[3] Buzási, A., Simões, S. G., Salvia, M., Eckersley, P., Geneletti, D., Olazabal, M., Wejs, A., Heidrich, O., Church, J. M., Pietrapertosa, F., De Gregorio Hurtado, S., Rivas, S., Fokaides, P., Ioannou, B. I., Feliu, E., Vasilie, S., Rekevičius, M., Matosović, M., Flamos, A., … Reckien, D. (2024). European patterns of local adaptation planning: A regional analysis. Regional Environmental Change, 24, 59. https://doi.org/10.1007/s10113-024-02211-w

[4] Caumo, S., Schramm, A., Oliveira Júnior, E. S., Girotto de Almeida Pina, C. S., Ignotti, E., Gioda, A., Massone, C. G., Pequeno de Araújo, L., Carreira, R., & Hacon, S. (2026). Background exposure to smoke-related pollutants among firefighters during training in the Pantanal biome. Revista Brasileira de Saúde Ocupacional, 51, e12. https://doi.org/10.1590/2317-6369/12024en2026v51e12

[5] Gasparrini, A., Guo, Y., Hashizume, M., Lavigne, E., Zanobetti, A., Schwartz, J., Tobias, A., Tong, S., Rocklöv, J., Forsberg, B., Leone, M., De Sario, M., Bell, M. L., Guo, Y.-L. L., Wu, C.-F., Kan, H., Yi, S.-M., de Sousa Zanotti Stagliorio Coelho, M., Saldiva, P. H. N., … Armstrong, B. (2015). Mortality risk attributable to high and low ambient temperature: A multicountry observational study. The Lancet, 386(9991), 369-375. https://doi.org/10.1016/S0140-6736(14)62114-0

[6] Giglio, L., Boschetti, L., Roy, D. P., Humber, M. L., & Justice, C. O. (2018). The Collection 6 MODIS burned area mapping algorithm and product. Remote Sensing of Environment, 217, 72-85. https://doi.org/10.1016/j.rse.2018.08.005

[7] Hamed, K. H., & Rao, A. R. (1998). A modified Mann-Kendall trend test for autocorrelated data. Journal of Hydrology, 204(1-4), 182-196. https://doi.org/10.1016/S0022-1694(97)00125-X

[8] Lawrence, M. G. (2005). The relationship between relative humidity and the dewpoint temperature in moist air: A simple conversion and applications. Bulletin of the American Meteorological Society, 86(2), 225-234. https://doi.org/10.1175/BAMS-86-2-225

[9] Lazaro, W. L., Oliveira-Júnior, E. S., Silva, C. J., Castrillon, S. K. I., & Muniz, C. C. (2020). Climate change reflected in one of the largest wetlands in the world: An overview of the Northern Pantanal water regime. Acta Limnologica Brasiliensia, 32, e104. https://doi.org/10.1590/s2179-975x7619

[10] MapBiomas Project. (2025). Annual land cover and land use maps of Brazil. https://brasil.mapbiomas.org

[11] Marengo, J. A., Alves, L. M., & Torres, R. R. (2016). Regional climate change scenarios in the Brazilian Pantanal watershed. Climate Research, 68(2-3), 201-213. https://doi.org/10.3354/cr01324

[12] Morin, C. W., Semenza, J. C., Trtanj, J. M., Glass, G. E., Boyer, C., & Ebi, K. L. (2018). Unexplored opportunities: Use of climate- and weather-driven early warning systems to reduce the burden of infectious diseases. Current Environmental Health Reports, 5(4), 430-438. https://doi.org/10.1007/s40572-018-0221-0

[13] Muñoz-Sabater, J., Dutra, E., Agustí-Panareda, A., Albergel, C., Arduini, G., Balsamo, G., Boussetta, S., Choulga, M., Harrigan, S., Hersbach, H., Martens, B., Miralles, D. G., Piles, M., Rodríguez-Fernández, N. J., Zsoter, E., Buontempo, C., & Thépaut, J.-N. (2021). ERA5-Land: A state-of-the-art global reanalysis dataset for land applications. Earth System Science Data, 13(9), 4349-4383. https://doi.org/10.5194/essd-13-4349-2021

[14] Rahman, M. M., McConnell, R., Schlaerth, H., Ko, J., Silva, S., Lurmann, F. W., Palinkas, L., Johnston, J., Hurlburt, M., Yin, H., Ban-Weiss, G., & Garcia, E. (2022). The effects of coexposure to extremes of heat and particulate air pollution on mortality in California: Implications for climate change. American Journal of Respiratory and Critical Care Medicine, 206(9), 1117-1127. https://doi.org/10.1164/rccm.202204-0657OC

[15] Requia, W. J., Amini, H., Mukherjee, R., Gold, D. R., & Schwartz, J. D. (2021). Health impacts of wildfire-related air pollution in Brazil: A nationwide study of more than 2 million hospital admissions between 2008 and 2018. Nature Communications, 12, 6555. https://doi.org/10.1038/s41467-021-26822-7

[16] Rocha, R., & Sant'Anna, A. A. (2022). Winds of fire and smoke: Air pollution and health in the Brazilian Amazon. World Development, 151, 105722. https://doi.org/10.1016/j.worlddev.2021.105722

[17] Sheehan, D., Mullan, K., West, T. A. P., & Semmens, E. O. (2024). Protecting life and lung: Protected areas affect fine particulate matter and respiratory hospitalizations in the Brazilian Amazon biome. Environmental and Resource Economics, 87(1), 45-87. https://doi.org/10.1007/s10640-023-00813-2

[18] Shen, S., Li, C., van Donkelaar, A., Jacobs, N., Wang, C., & Martin, R. V. (2024). Enhancing global estimation of fine particulate matter concentrations by including geophysical a priori information in deep learning. ACS ES&T Air, 1(5), 332-345. https://doi.org/10.1021/acsestair.3c00054

[19] Silveira, G. O., Brum, R. L., Tavella, R. A., Bonifácio, A. S., Fernandes, R. C., & Silva Júnior, F. M. R. (2026). Impact of PM2.5 on cardiorespiratory mortality: A study in the capitals of Brazilian Amazon rainforest. Toxicology, 521, 154401. https://doi.org/10.1016/j.tox.2026.154401

[20] Sobreira, E., Pereira, T. F., Dias, D. F., Viana, C. R. S., de Paula, J. S. B. C., Barbosa, A. P. D., de Souza, A. R., da Rocha Pedra, T., dos Santos, M. C., de Souza Campos, D. V., Romano, A. M., Kosten, S., Muniz, C. C., Ikeda-Castrillon, S. K., & Lázaro, W. L. (2025). Human pressure on the Pantanal: A four-decade analysis of land cover changes, ecological degradation, and future prospects. In T. Pullaiah (Ed.), Wetlands of Tropical and Subtropical South and Central America. Wiley. https://doi.org/10.1002/9781394307166.ch05

[21] Thielen, D., Schuchmann, K.-L., Ramírez-Ramírez, P., Marquez, M., Rojas, W., Quintero, J. I., & Marques, M. I. (2020). Quo vadis Pantanal? Expected precipitation extremes and drought dynamics from changing sea surface temperature. PLOS ONE, 15(1), e0227437. https://doi.org/10.1371/journal.pone.0227437

[22] World Health Organization. (2021). WHO global air quality guidelines: Particulate matter (PM2.5 and PM10), ozone, nitrogen dioxide, sulfur dioxide and carbon monoxide. World Health Organization. https://iris.who.int/handle/10665/345329

https://doi.org/10.12974/2311-8741.2026.14.05